



## A NON-LINEAR EIGENVALUE PROBLEM ASSOCIATED WITH INEXTENSIBLE WHIRLING STRINGS

J. COOMER, M. LAZARUS AND R. W. TUCKER

*Department of Physics, University of Lancaster, Bailrigg, Lancaster, LA1 4YB, England.*

*E-mail: r.tucker@lancaster.ac.uk*

D. KERSHAW

*Department of Mathematics, University of Lancaster, Bailrigg, Lancaster, LA1 4YB, England.*

*E-mail: d.kershaw@lancaster.ac.uk*

AND

A. TEGMAN

*Department of Physics, Faculty of Science, Ankara University, Ankara 065100, Turkey*

*(Received 8 March 1999, and in final form 19 May 2000)*

The motion of idealized inextensible strings is discussed. The equations of motion are analyzed for closed-loop configurations, free of body forces and open hanging strings whirling under gravity. The latter give rise to an interesting non-linear eigenvalue problem describing a spectrum of *whirling* modes that is amenable to numerical investigation by using the *shooting* method for two-point boundary value problems. The spectrum is compared with that for small amplitude excitations in both fixed and rotating vertical plane through the suspension point. The results provide a useful theoretical background for an analysis of a laboratory exploration of *whirling* chains.

© 2001 Academic Press

### 1. INTRODUCTION

A common introduction to wave motion and the normal mode analysis of a one-dimensional continuum is via the study of small oscillations of an idealized elastic string. With appropriate assumptions a linear wave equation is readily derived and its analysis is a natural precursor to the study of wave propagation in a multitude of other systems of relevance in Nature. However, such an idealization may not offer any guidance for tackling situations where disturbances are not necessarily small compared with the dimensions of the system. In large-amplitude oscillations of a real string the longitudinal and transverse motions become coupled and a realistic treatment relies on a careful consideration of the appropriate *constitutive relations* linking the configuration of the system to the elastic forces exerted by the medium [1–3]. Such considerations become mandatory if one is to distinguish the behaviour of a rubber band from that of a violin string. The constitutive relations for such realistic systems generally give rise to a non-linear wave equation [4]. There is also a class of problems where the elastic forces are provided by the constraint of *inextensibility* [5–7]. Such problems clearly lie outside the scope of treatments rooted in the use of Hooke's law. It is the purpose of this note to explore at

a pedagogical level the rich dynamical structure inherent in the motion of inextensible homogeneous strings or chains hanging from a fixed point under gravity or whirling as loops freely in space.

If one rolls the end of a small length of cotton thread between finger and thumb it can be made to execute an interesting whirling motion. A similar phenomenon is readily visible by twiddling a key chain in a similar manner. The nature of the whirling configuration depends on its mode of excitation, particularly its angular speed. Similar configurations are possible with longer hanging ropes, cords, or chains. These are the examples of the dynamical systems that are discussed here, idealized as one-dimensional inextensible material media. Motion with one point fixed, under Earth's uniform gravitational field is considered first. It is assumed that the medium can sustain a *contact tension* directed along its length during every moment of its motion and will be referred to as a *string* or *chain* for short. Periodic boundary conditions are then described for a class of interesting axial motions executed by closed loops in the absence of body forces.

Since physical media are never truly one-dimensional or strictly inextensible the system under discussion is an idealization. However, it is a different idealization from the discussion of a Hookean elastic string executing small vibrations and one cannot *a priori* assert that the *tension* along its length remains constant in time irrespective of its dynamical configuration. The magnitude of the tension arises dynamically from the inextensibility assumption and must be determined from the equations of motion along with the configuration of the system as a function of time. It is this particular feature that is emphasized in the following treatment.

In section 2 the general equations of motion for such a system are established. In section 3 the analytic form of the general solution for a hanging string executing *small vibrations in a fixed plane* are written down before discussing the normal modes appropriate for the description of *whirling modes of large amplitude in a rotating plane* in section 4. The behaviour of whirling modes is of direct relevance to a number of important industrial processes ranging from the dynamics of drill-strings in the oil exploration industry [8] to the control of balloon formation in the spinning of yarn [9, 10]. As will be seen, the analysis of general whirling solutions can give rise to an interesting non-linear eigenvalue problem in contrast to the linear eigenvalue problem for motions with small amplitude. A number of techniques designed to elucidate the large-amplitude motion of the system are suggested. For closed loops the imposition of periodicity leads to novel *spinning configurations* and analytic expressions are obtained for flowing circular motions in the absence of net external body forces. In the final section, numerical results are discussed, suggestions offered for the excitation and detection of whirling eigenmodes in the laboratory and the theoretical analysis compared with observations on realistic chains.

## 2. EQUATION OF MOTION FOR AN INEXTENSIBLE MATERIAL STRING

Suppose the elements of an inextensible string are labelled by a variable  $s$  that runs from  $s = 0$  to  $L$  where  $L$  is its length. Let  $\rho(s)$  denote its mass per unit length. With reference to an arbitrary origin in space denote the position of such elements at time  $t$  by the vector  $\mathbf{r}(s, t)$ . Thus, at time  $t = t_0$  the space curve  $s \mapsto \mathbf{r}(s, t_0)$  is the instantaneous configuration of the string in an inertial frame. Since the length of the string is  $\int_0^L \sqrt{\partial_s \mathbf{r} \cdot \partial_s \mathbf{r}} ds$  the condition

$$\partial_s \mathbf{r} \cdot \partial_s \mathbf{r} = 1 \tag{1}$$

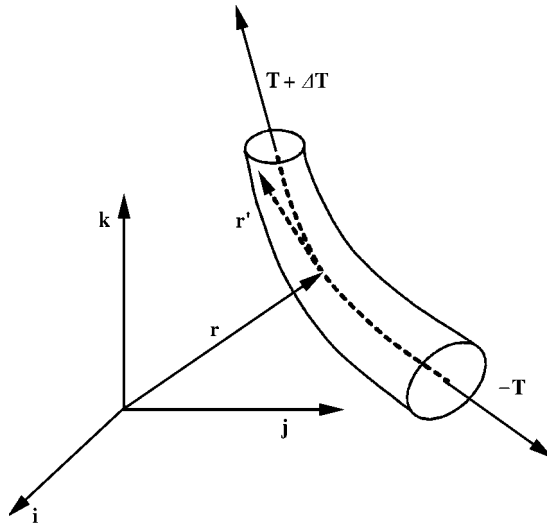


Figure 1. For a string or chain the elastic contact forces are directed along a tangent to the (dotted) line of centroids. The figure shows the location of an element of material in a global Cartesian frame of reference. Its motion is determined by the difference in the vector tension between its extremities.

implies that  $s$  measures arc-length along the string. The condition that the string is inextensible means that relation (1) must be maintained at all time. Clearly,  $\partial_s \mathbf{r} \equiv \mathbf{r}_s$  is a unit vector (see Figure 1) and one may write the vector tension in the string as

$$\mathbf{T}(s, t) = T(s, t)\mathbf{r}_s \tag{2}$$

in terms of its magnitude  $T(s, t)$ . As stressed above for idealized inextensible strings this tension is a dynamical variable that must be determined along with  $\mathbf{r}(s, t)$  from the equations of motion, initial and boundary conditions. The net tension force that accelerates an element  $d\mathbf{r}$  of the string is, to first order in  $ds$

$$\{\mathbf{T}(s, t) + \partial_s \mathbf{T}(s, t) ds\} - \mathbf{T}(s, t), \tag{3}$$

while gravity contributes a body force  $\rho(s)ds\mathbf{g}$ , where  $\mathbf{g}$  is the vector acceleration due to gravity. Since  $\rho(s) ds \dot{\mathbf{r}}(s, t)$  is the momentum of the element, Newton's law gives

$$\rho \partial_{tt} \mathbf{r} = \rho \mathbf{g} + \partial_s (T\mathbf{r}_s). \tag{4}$$

Equations (1) and (4) together with initial and boundary conditions are to be solved for  $\mathbf{r}(s, t)$  and  $T(s, t)$ . Solutions corresponding to one end of the string constrained to be fixed in space while the other end is free are explored first. Thus, the tension must be zero at the free end.

Equations (1) and (4) constitute four coupled non-linear partial differential equations in two independent variables. In the following, material with a uniform density  $\rho(s) = \rho_0$  is considered. It is convenient to introduce dimensionless quantities by using the transformations  $\tau = t/t_0$ ,  $\sigma = s/L$ ,  $\mathbf{R}(\sigma, \tau) = \mathbf{r}(s, t)/L$ ,  $\mathbf{h} = \mathbf{g}t_0^2/L$ ,  $\mathcal{T}(\sigma, \tau) = T(s, t)t_0^2/(L^2\rho_0)$ , where  $t_0$  is an arbitrary scale with the dimensions of time. In the following  $t_0^2 = L/g$  where  $g = |\mathbf{g}|$ .

Then the dimensionless equations of motion are

$$\mathbf{R}_\sigma \cdot \mathbf{R}_\sigma = 1, \quad \partial_{\tau\tau}\mathbf{R} = \mathbf{h} + \partial_\sigma(\mathcal{F} \partial_\sigma \mathbf{R}), \tag{5, 6}$$

and note that  $0 \leq \sigma \leq 1$ . Choose Cartesian co-ordinates so that the  $x$ - and  $y$ -axis are horizontal while the  $z$ -axis is directed downwards from the origin so that  $\mathbf{h} = (0, 0, 1)$ . With  $\mathbf{R}(\sigma, \tau) = (x(\sigma, \tau), y(\sigma, \tau), z(\sigma, \tau))$ , equations (5) and (6) give

$$(\partial_\sigma x)^2 + (\partial_\sigma y)^2 + (\partial_\sigma z)^2 = 1, \tag{7}$$

$$\partial_{\tau\tau}x = \partial_\sigma(\mathcal{F} \partial_\sigma x), \quad \partial_{\tau\tau}y = \partial_\sigma(\mathcal{F} \partial_\sigma y), \quad \partial_{\tau\tau}z = 1 + \partial_\sigma(\mathcal{F} \partial_\sigma z). \tag{8-10}$$

For a string hung from the (fixed) origin ( $\sigma = 1$ ) with the free end at  $\sigma = 0$ , the boundary conditions are  $\mathbf{R}(1, \tau) = 0, \mathcal{F}(0, \tau) = 0$ .

### 3. MOTION IN A FIXED PLANE

Equations (7)–(10) constitute a non-linear system of partial differential equations for the general history of the space curve  $\mathbf{R}(\sigma, \tau)$ . One strategy to solve these equations is to seek configurations that reduce this system to ordinary differential equations. Guided by physical intuition one expects that the hanging string will admit vibrations in both a fixed and rotating vertical plane in space. Both cases lend themselves readily to approximate treatments if the amplitude of oscillation is maintained small compared with the physical length of the string. It is instructive to analyze these approximations first since it will be noted in section 4 how they relate to the larger *whirling* motions in which the plane of vibration rotates uniformly about a vertical axis through the point of suspension.

Clearly, equations (7)–(10) admit solutions with, say  $y(\sigma, \tau) = 0$  corresponding to motion in the fixed  $z$ - $x$  plane. Furthermore, if the motion is such that  $|\partial_\sigma x(\sigma, \tau)| \ll 1$  for all  $\tau$  so that equation (7) is satisfied to a good approximation by

$$z(\sigma, \tau) = 1 - \sigma, \tag{11}$$

where the constant ensures that  $z(1, \tau) = 0$ , then equation (10) implies  $\partial_\sigma \mathcal{F}(\sigma, \tau) = 1$ . Since  $\mathcal{F}(0, \tau) = 0$  one must have

$$\mathcal{F}(\sigma, \tau) = \sigma. \tag{12}$$

Inserting this in equation (8) yields

$$\partial_{\tau\tau}x = \partial_\sigma(\sigma \partial_\sigma x), \tag{13}$$

whose general solution (regular at  $\sigma = 0$ ) is a superposition of eigenmodes of the form

$$x(\sigma, \tau) = \sum_{k=1}^{\infty} A_k J_0(\mu_k \sqrt{\sigma}) \sin(\frac{1}{2} \mu_k \tau + \phi_k) \tag{14}$$

in terms of the Bessel function  $J_0$ . The amplitudes  $A_k$  and phases  $\phi_k$  may be determined from the initial conditions  $x(\sigma, 0)$  and  $\partial_\tau x(\sigma, 0)$  while the characteristic eigenfrequencies of small oscillations are determined by the boundary condition  $x(1, \tau) = 0$  and correspond to the

infinite number of roots of the equation

$$J_0(\mu) = 0. \tag{15}$$

The approximate solution indicates that the  $k$ th eigenmode vanishes at points determined by  $\sigma = \sigma_r^k$  where  $J_0(\mu_k \sqrt{\sigma_r^k}) = 0$ . Since the roots  $\mu_k$  are distinct and start from  $\mu_1$  this implies the existence of  $k$  nodes determined by

$$\sigma_r^k = (\mu_r/\mu_k)^2, \quad r = 1, \dots, k. \tag{16}$$

#### 4. WHIRLING CONFIGURATIONS

In the previous section, one continuous degree of freedom was frozen by restricting motion to a *fixed* plane in space. In this section, a class of solutions obtained by restricting the motion to a uniformly *rotating* plane in space is examined. An element of the hanging string, labelled by  $\sigma = \sigma_0$ , that moves in a horizontal circle of radius  $\chi_0$  with angular frequency  $\omega/t_0$  rad/s at a height given by  $z = z_0$  describes the space curve ( $x = \chi_0 \cos(\omega\tau)$ ,  $y = \chi_0 \sin(\omega\tau)$ ,  $z = z_0$ ). This suggest that one search for *whirling* solutions of the form

$$\mathbf{R}(\sigma, \tau) = (\chi(\sigma) \cos(\omega\tau), \quad \chi(\sigma) \sin(\omega\tau), \quad \zeta(\sigma)), \quad \mathcal{T}(\sigma, \tau) = \mathcal{T}_0(\sigma), \tag{17, 18}$$

with  $\mathcal{T}_0(0) = 0$ . The components of  $\mathbf{R}$  are specified with respect to a Cartesian inertial frame. This corresponds to a time independent configuration when viewed with respect to a vertical plane rotating with a fixed angular speed  $\Omega = \omega \sqrt{g/L}$  rad/s about a vertical axis that passes through the suspension point. Inserting equations (17) and (18) into equations (7)–(10) shows that the functions  $\chi$ ,  $\zeta$  and  $\mathcal{T}_0$  must satisfy

$$\partial_\sigma(\mathcal{T}_0 \partial_\sigma \chi) = -\omega^2 \chi, \quad \partial_\sigma(\mathcal{T}_0 \partial_\sigma \zeta) = -1, \quad (\partial_\sigma \chi)^2 + (\partial_\sigma \zeta)^2 = 1, \tag{19-21}$$

with  $\chi(1) = \zeta(1) = 0$ , and the equations of motion are reduced to a system of coupled ordinary differential equations. Clearly equations (19) and (20) express a balance of tensile forces with centrifugal and gravitational forces, respectively, in a non-inertial co-ordinate system while equation (21) maintains the inextensibility constraint.

Following the tactics in section 3 consider first small deflection of the string from the vertical with  $(\partial_\sigma \chi)^2 \ll 1$  so that equation (21) is satisfied with  $\zeta(\sigma) = 1 - \sigma$ . The tension now follows by integrating equation (20) with  $\mathcal{T}_0(0) = 0$ :

$$\mathcal{T}_0(\sigma) = \sigma. \tag{22}$$

Inserting this into equation (19) gives

$$\partial_\sigma(\sigma \partial_\sigma \chi) + \omega^2 \chi = 0 \tag{23}$$

for eigenfunctions  $\chi$  satisfying  $\chi(0) = 0$ . Such eigenfunctions are given in terms of the 0th order Bessel function,

$$\chi_k(\sigma) = J_0(2\omega_k \sqrt{\sigma}), \tag{24}$$

where the eigenspeeds  $\{\omega_k\}$  are determined from the boundary condition to be the roots of the equation

$$J_0(2\omega_k) = 0. \tag{25}$$

According to this linearized approximation each eigenfunction is associated with a particular whirling eigenspeed  $\omega_k$ . It will be noticed that this set of whirling eigenspeeds coincides with the angular frequencies of small planar oscillations  $\{\mu_k/2\}$  discussed in the previous section. The *small amplitude* whirling modes appear as a superposition of such planar oscillations in a rotating plane. This solution also implies that only a discrete set of stationary whirling speeds above a non-zero minimum ( $\omega_1$ ) is permitted, contrary to the experience.

By contrast to the linearized analysis one may now proceed to analyze equations (19)–(21) making no assumptions about the size of the possible displacements. One may immediately integrate equation (20) to get

$$\mathcal{T}_0 \partial_\sigma \zeta = -\sigma, \tag{26}$$

since  $\mathcal{T}_0(0) = 0$ . Introduce

$$u(\sigma) = \mathcal{T}_0(\sigma) \partial_\sigma \chi(\sigma) \tag{27}$$

into equations (21) and (26) so that

$$\mathcal{T}_0 = \sqrt{u^2 + \sigma^2}. \tag{28}$$

Using this to integrate equation (26) gives

$$\zeta(\sigma) = - \int_1^\sigma \frac{s ds}{\sqrt{u^2(s) + s^2}}, \tag{29}$$

satisfying  $\zeta(1) = 0$ . Similarly, equation (27) yields

$$\chi(\sigma) = \int_1^\sigma \frac{u(s) ds}{\sqrt{u^2(s) + s^2}}, \tag{30}$$

satisfying  $\chi(1) = 0$ . Inserting equation (27) into equation (19) yields

$$\partial_\sigma(u) = -\omega^2 \chi \tag{31}$$

and differentiating this gives finally

$$\frac{d^2 u}{d\sigma^2} + \lambda \frac{u}{\sqrt{u^2 + \sigma^2}} = 0, \tag{32}$$

where  $\lambda = \omega^2$ . In terms of  $u$  the free end boundary condition  $\mathcal{T}_0(0) = 0$  is

$$u(0) = 0. \tag{33}$$

At the origin,  $\chi(1) = 0$  so equation (31) implies

$$\partial_\sigma u(1) = 0. \tag{34}$$

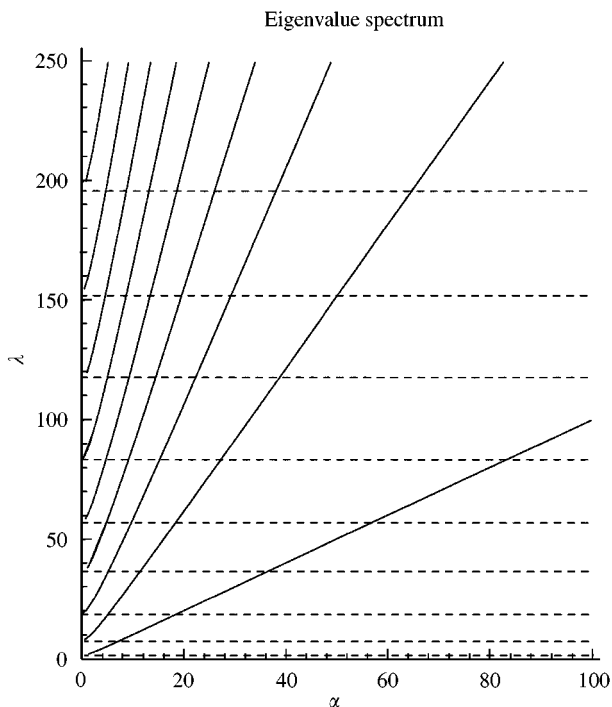


Figure 2. Eigenvalues  $\lambda = \omega^2$  as a function of the configurational shooting parameter  $\alpha$  associated with the motion of an inextensible string whirling with angular speed  $\omega$  under gravity. Each line designates a possible mode associated with the pair  $(\alpha, \lambda)$  on it. The dotted horizontal lines denote the analogous predictions of the linearized theory for small whirling amplitudes..

Equation (32) together with equations (33) and (34) constitute a non-linear eigenvalue problem for  $u(\sigma)$  [11]. Each eigenvalue  $\lambda$  and associated eigenfunction  $u(\sigma)$  determines via equations (29) and (30) the configuration  $\chi(\sigma), \zeta(\sigma)$  together with the corresponding reduced tension (28). Equations (32)–(34) do not have an immediate analytic solution. They are, however, amenable to numerical analysis. One notes that the boundary conditions consist of values of  $u$  specified at different points. Traditional numerical methods for solving second order ordinary differential equations require a specification of the function and its first derivative at the initial point of the integration range. Such methods may still be used to explore the non-linear eigenvalue problem here by exploiting the so-called *shooting method* [12, 13]. In this problem choose as initial data  $(u(0) = 0, \partial_\sigma u(0) = \alpha)$  for some arbitrary number  $\alpha$ . For a particular choice of (positive)  $\lambda$ , equation (32) is then integrated from  $\sigma = 0$  to  $\sigma = 1$  where  $\partial_\sigma u(1)$  is compared with zero. If  $|\partial_\sigma u(1)|$  is not within some small assigned distance from zero the initial value of  $\alpha$  is adjusted and the integration is repeated. When this approach is used to integrate equation (32) an interesting result emerges. For any given choice of  $\lambda$  in general several values of  $\alpha$  arise for which the boundary conditions are satisfied. Thus, each  $\alpha$  generates a distinct configuration of the whirling string associated with a particular whirling frequency. There is a Maple programme written by Douglas Meade available in the Maple V share library designed to solve two-point boundary value problems of the type under discussion [14]. With the aid of this programme the eigenstructure of equation (32) has been explored up to  $\lambda = 250$  and the results are displayed in Figure 2. The programme can be placed in a simple loop which increments the value of  $\alpha$  through a range for a particular value of  $\lambda$ . Thus, for  $\lambda = 100$  the programme

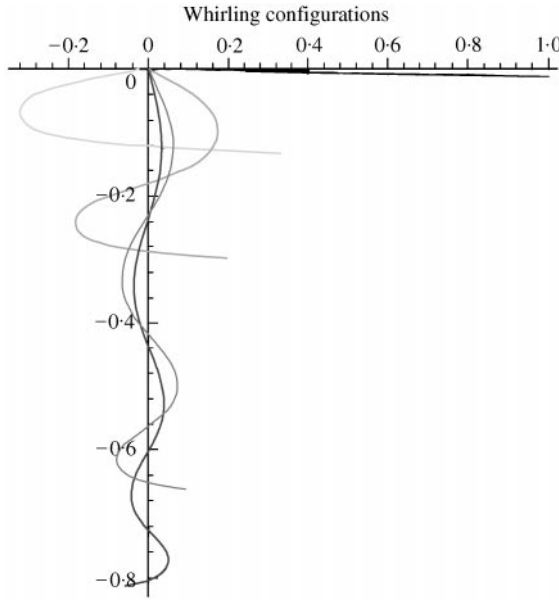


Figure 3. A selection of whirling configurations corresponding to  $\lambda = 150$  as predicted by the shooting method of solution to the non-linear eigenvalue problem described in the text.

returns six values for  $u(s)$  each with a different starting value of  $\alpha$  and increasing the loop increment or the range of  $\alpha$  produces no more solutions. It is clear that the degeneracy of solutions (i.e., the number of distinct whirling configurations with the same whirling frequency) increases with whirling speed. Different whirling configurations with the same whirling speed are distinguished by having different numbers of nodes (defined as those points where the string intersects the vertical). In Figure 2 the horizontal lines locate the eigenvalues in the linearized description. Unlike in the linearized theory there is now a particular (family) of possible eigenmodes associated with any non-zero whirling speed  $\omega$ . For each solution one can plot the configuration of the chain in the co-rotating plane. The corresponding tension as given by equation (28) can be similarly displayed. Figure 3 displays a family of degenerate whirling configurations corresponding to  $\lambda = 150$ . Figure 4 displays a particular whirling mode (dotted) corresponding to  $\lambda = 100$  together with the associated variation of the scaled tension. It is of interest to note that the minima and maxima of the tension occur at the nodes and the extrema of the spatial configuration respectively.

Further insight may be obtained by recasting the equations of motion into first order form. The derivatives of equations (29) and (30) together with equation (31) give

$$\frac{d}{ds} \mathbf{F}(s) = \mathbf{H}(s, \lambda), \tag{35}$$

where

$$\mathbf{F} = (u(s), \zeta(s), \chi(s)), \tag{36}$$

$$\mathbf{H} = (-\lambda\chi(s), -s/\sqrt{u(s)^2 + s^2}, u(s)/\sqrt{u(s)^2 + s^2}). \tag{37}$$



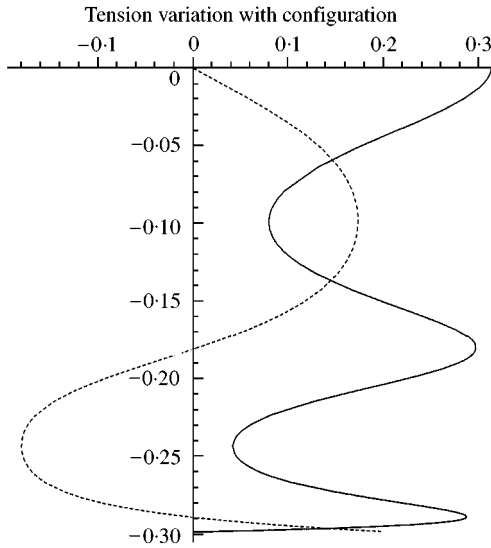


Figure 4. A whirling configuration (····) corresponding to  $\lambda = 100$  together with the variation of the (—) scaled reduced tension  $\tau$  in the chain along its length as predicted by the shooting method of solution to the non-linear eigenvalue problem described in the text.  $\tau$  has been scaled by 0.9 in order to display it on the same picture. Note that the minima of the tension occur at the extrema of the whirling configuration and the maxima of the tension occur at the nodes.

For a given  $\lambda$  equation (35) can be integrated with initial conditions  $\mathbf{F}(0, \zeta_0, \chi_0)$  and  $\zeta_0, \chi_0$  adjusted until equation (34) is satisfied. In this approach it is clear how different positions of the free end of the whirling string can be adjusted to satisfy the boundary conditions for any given whirling speed.

As an alternative to the numerical integration of the differential equations above one may contemplate a variational approach. Multiplying equation (32) by  $u(s)$  and integrating over the  $\sigma$  domain yields

$$\int_0^1 u \partial_{\sigma\sigma} u \, d\sigma + \lambda \int_0^1 \frac{u^2 \, d\sigma}{\sqrt{\sigma^2 + u^2}} = 0. \tag{38}$$

Integrating the first term by parts and using the boundary conditions (33) and (34) gives

$$\lambda = A[u],$$

where

$$A[u] = \int_0^1 (\partial_{\sigma} u)^2 \, d\sigma \bigg/ \int_0^1 \frac{u^2 \, d\sigma}{\sqrt{\sigma^2 + u^2}}. \tag{39}$$

This suggests that  $\lambda$  can be generated from a local extremum of the numerator of equation (39) subjected to some constraint. Indeed one may readily find a Lagrangian  $\mathcal{L}$  for equation (32):

$$\mathcal{L}(\partial_{\sigma} u, u, s) = \frac{1}{2} (\partial_{\sigma} u)^2 - \lambda \sqrt{u^2 + \sigma^2}. \tag{40}$$

From equations (31) and (27) it follows that the energy  $\int_0^1 \mathbf{R}^2 \, d\sigma$  is being minimized subject to keeping the integrated tension  $\int_0^1 \sqrt{u^2 + \sigma^2} \, d\sigma$  constant. If one chooses an  $N$  parameter

trial function  $u^N(a_1, \dots, a_N, \sigma)$  satisfying equations (33) and (34) then  $\lambda$  may be estimated from equation (39) by solving

$$\partial_{a_j} A[u^N] = 0 \quad (41)$$

for the parameters  $a_j, j = 1, \dots, N$ .

It is clear from equations (7)–(10) that a more symmetric system of equations arises in the case  $\mathbf{g} = 0$ . This could be achieved by taking the string into a gravity free domain or by subjecting it to additional body forces that cancel  $\mathbf{g}$ , such as those produced by an external electromagnetic field. On physical grounds one would then expect the existence of configurations in which planar circular loops of chain rotate about an axis through the centre of each circle perpendicular to its plane. For such problems the two-point boundary condition above is replaced by the periodicity condition  $\mathbf{R}(\sigma, \tau) = \mathbf{R}(\sigma + 1, \tau)$ . Upon choosing the plane containing the circle to be  $z = 0$  it is easy to verify that, despite the non-linear nature of the differential equations, an exact solution describing such a configuration exists. It is given by

$$x(\sigma, \tau) = R_0 \cos(2\pi(\sigma + v\tau)), \quad (42)$$

$$y(\sigma, \tau) = R_0 \sin(2\pi(\sigma + v\tau)), \quad (43)$$

$$z(\sigma, \tau) = 0, \quad T(\sigma, \tau) = v^2, \quad (44, 45)$$

where  $R_0 = 1/2\pi$  and the constant  $v$  describes the (reduced) circumferential speed of a point of the chain. What is less intuitive is that solutions of a similar nature exist in which the chain “flows” in closed loops of *arbitrary shape*. A discussion of these interesting configurations and their stability under deformation can be found in reference [15].

## 5. DISCUSSION

From Newton’s equations of motion for an inextensible hanging chain the equations describing small amplitudes oscillations in both a fixed and a rotating plane have been deduced. These may be contrasted with free rotating loops and whirling configurations under gravity of large amplitude. The whirling modes arise as solutions to a non-linear differential equation that is solved subject to a two-point boundary condition. Such a non-linear eigenvalue problem is amenable to numerical analysis by either the *shooting method* or variational techniques. The former has been used to elucidate the spectrum in this article. It is believed that the solutions offer valuable insight into a number of important concepts including the role of the inextensibility constraint, linearization, the superposition of solutions and the concept of degeneracy. They also offer an introduction to more advanced concepts relating the behaviour of linearized solutions to general solutions described by a parameter ( $\lambda$ ). Indeed, parts of Figure 2 relate to bifurcations in the theory of whirling strings [4]. For any whirling speed  $\Omega$  rad/s, with  $\lambda$  corresponding to  $\Omega^2 Lg$ , the whirling eigenmodes lie on the full lines in Figure 2. The dotted horizontal lines denote the analogous predictions of the linearized theory for small whirling amplitudes and it will be noted how the predictions of the linearized theory depart from the full theory as the whirling amplitudes (as measured by  $\alpha$ ) increase.

The theoretical analysis above offers a valuable background for an experimental investigation into the behaviour of realistic hanging chains excited by rotary motion.

According to Figure 2, if  $\lambda_n$  denotes one of the infinite set of ordered eigenvalues associated with the whirling modes of small amplitude then for any  $\lambda \equiv \omega^2$  between  $\lambda_n$  and  $\lambda_{n+1}$  there is a set of  $n$  whirling configurations  $\{\mathbf{R}_1^{(\lambda)}, \mathbf{R}_2^{(\lambda)}, \dots, \mathbf{R}_n^{(\lambda)}\}$ . For an inextensible chain the total energy of each whirling configuration is the sum of its kinetic and gravitational potential energies and is readily shown to vary linearly with  $\lambda$ . If one counts the suspension point as a node then the configuration given by  $\mathbf{R}_k^{(\lambda)}$  has  $k$  nodes. In an attempt to confront the predictions of this idealized model with the behaviour of real whirling chains a small experimental rig has been constructed that can suspend chains with lengths of order 1–2 m and excite them into rotary motion with the aid of a variable speed DC electric motor.

However, notwithstanding the caveats mentioned in section 2 it is by no means trivial to excite a pure whirling eigenmode in a hanging chain and some ingenuity is required in order to compare the theory discussed above with observations on real chains. Following some of the suggestions in reference [7] a combination of stroboscopic techniques and flash photography can be used to explore the configuration of a chain driven by a variable speed DC motor at its upper end. By carefully varying the rotation speed of the motor driving suitably flexible chains it is possible to verify the existence of whirling configurations closely approximating those predicted by the shooting programme and by counting the nodes as a function of the motor speed the general features of the eigenvalue spectrum can be explored.

One of the main problems in observing whirling eigenmodes in a chain few metres long is the inevitable dynamical coupling between different whirling modes induced by extraneous vibration from the drive source and frictional effects (including viscoelasticity in the chain). Much of the extraneous vibration produced by the electric motor excites non-stationary interference effects that are readily observed under strong illumination. Such effects can be reduced by damping the axial and lateral vibrations where the chain is attached to the rotary drive. This may be achieved by connecting the drive shaft of the motor to the chain by means of a stiff plastic coupler. In order to excite different whirling modes it was found expedient to touch the whirling chain (with a rigid rod) at some point along its length. By judiciously choosing the point of contact a particular eigenmode can be encouraged to form. Such modes typically exist for several seconds before becoming contaminated with other dynamical structure. The photographic plate (Figure 5) clearly shows the profile of a typical whirling configuration captured by flash photography. In this manner, one may correlate the number of characteristic nodes in the pure whirling configuration with the ambient whirling speed. According to the solutions displayed in Figure 2, a finite number of such configurations are possible for any whirling speed. In practice, it is often found that a particular set of configurations are dominant with some apparently absent entirely. Despite this shortcoming, no whirling eigenmode was ever observed with more nodes than those predicted by the idealized model analyzed in this paper. A typical set of data is displayed in Figure 6 where the number of observed nodes is displayed against the whirling speed in Hz (1 Hz = 60 RPM =  $2\pi$  rad/s) for a chain of length 0.764 m. With  $g = 9.81$  m/s/s the relation between  $\lambda$  and the whirling speed  $\Omega$  in rad/s for such a chain is,

$$\lambda = 0.08\Omega^2.$$

Comparing with Figure 2 one sees that at, say  $\Omega = 8\pi$ ,  $\lambda \simeq 51$  and (excluding the point of suspension) two of the three predicted low-frequency whirling modes were observed. In the range amenable to observation most of the predicted whirling modes with more than three nodes were observed, and no others.

The use of the scaled variables introduced in section 2 also makes it possible to investigate the (in)dependence of the motion on the mass density and length of the chain.

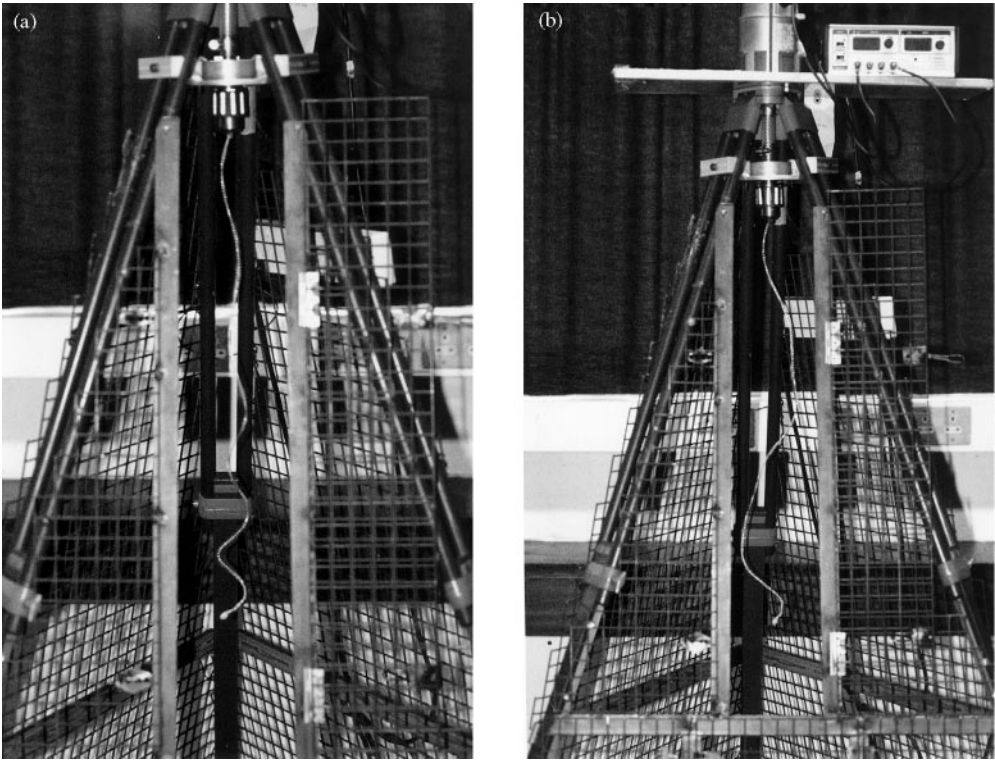


Figure 5. Experimentally observed whirling eigenmodes.

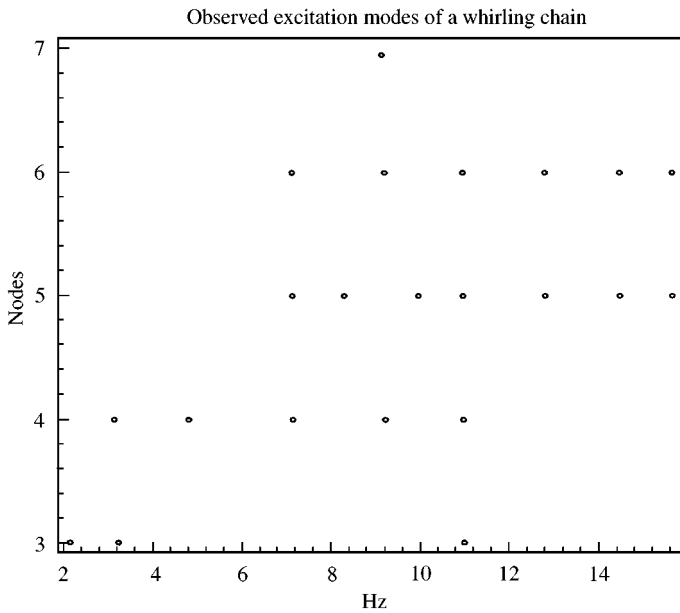


Figure 6. Experimentally observed whirling configurations for a chain of length 0.765 metres as a function of whirling speed (1 Hz) = 60 rpm). Each configuration is labelled by its number of nodes, excluding the point of suspension.

Since the theory above ignores internal dissipation of energy the use of different types of chain can be used to explore the realm of applicability for the idealized theory. Such observations lend credence to the theoretical analysis of the idealized inextensible whirling string and are in full accord with the existence proof given in reference [11]. They also offer an enhanced appreciation of a number of related concepts in the dynamics of inextensible strings.

## 6. CONCLUSION

An account has been given of certain motions of closed and open inextensible strings, modelled in terms of simple one dimensional continua under variable tension. In particular, a discussion has been given of the large amplitude whirling eigenmodes of a string suspended under gravity and the “flowing” modes of a closed string in the absence of gravity. The vibrational behaviour of the former has been contrasted with the linearized description. The non-linear eigenproblem for whirling modes has been solved numerically by using a “shooting” method for a range of whirling speeds and an attempt made to confront the numerical predictions with observation by using a small experimental rig. The results lend credence to the theoretical results despite the neglect of damping both along the structure and at its point of suspension.

## ACKNOWLEDGMENTS

RWT acknowledges the support from EPSRC. AT wishes to thank the Scientific and Technical Research Council of Turkey (TUBITAK) for a fellowship and is grateful to the Department of Physics, Lancaster University for providing hospitality. The authors are grateful to John O'Connor for drawing their attention to reference [9].

## REFERENCES

1. J. B. KELLER 1959 *American Journal of Physics* **27**, 584–586. Large amplitude motion of a string.
2. S. ANTMAN 1980 *American Mathematical Monthly* **87**, 359–370. The equation for large vibrations of strings.
3. N. J. ZABUSKY 1962 *Journal of Mathematical Physics* **3**, 1028–1039. Exact solution for the vibrations of a nonlinear continuous model string.
4. S. ANTMAN 1991 *Non-linear Problems in Elasticity*. Berlin: Springer, Applied Mathematical Sciences 107.
5. D. A. LEVINSON 1977 *American Journal of Physics* **45**, 680–681. Natural frequencies of a hanging chain.
6. J. P. MCCREESH, T. L. GOODFELLOW and A. H. SEVILLE 1975 *American Journal of Physics* **43**, 646–648. Vibrations of a hanging chain of discrete links.
7. A. B. WESTERN 1980 *American Journal of Physics* **48**, 54–56. Demonstration for observing  $J_0(x)$  on a resonant rotating vertical chain.
8. R. W. TUCKER and C. WANG 1999 *Journal of Sound and Vibration* **224**, 123–165. An integrated model for drill-string dynamics.
9. W. B. FRASER 1993 *Philosophical Transactions of Royal Society of London A* **342**, 439–468. On the theory of ring spinning.
10. F. ZHU, R. SHARMA and C. D. RAHN 1997 *ASME Journal of Applied Mechanics* **64**, 676–683. Vibrations of ballooning Elastic Strings.
11. I. KOLODNER 1955 *Communications in Pure and Applied Mathematics* **8**, 395–408. Heavy rotating string—a non-linear eigenvalue problem.

12. J. M. ORTEGA and W. G. POOL, JR 1981 *An Introduction to Numerical Methods for Differential Equations*. London: Pitman.
13. H. B. KELLER 1970. *Numerical Methods for Two-Point Boundary Problems*. New York: Blaisdell.
14. D. MEADE 1998. *A Maple implementation of the simple shooting method*. Department of Mathematics, University of South Carolina, Columbia, SC 29208, U.S.A.
15. T. J. HEALEY, 1990 *Quarterly Journal of Applied Mathematics* **48**, 679–698. Stability and bifurcation of rotating non-linearly elastic loops.